

# Chemical structure, water absorbency and thermal properties of poly(acrylamide-*co*-acrylic acid)-grafted-poly(styrene-*co*-methyl methacrylate) “raspberry” – shape like structure microgels

Ros Azlinawati Ramli<sup>1</sup>, Shahrir Hashim<sup>2</sup>, Waham Ashaier Laftah<sup>3</sup>

<sup>1</sup> Material Technology Program, Faculty of Industrial Sciences & Technology, Universiti Malaysia Pahang (UMP), 26300 Gambang, Kuantan, Pahang.

<sup>2</sup> Department of Polymer Engineering, Faculty of Chemical Engineering, Universiti Teknologi Malaysia (UTM), 81310 Skudai, Johor, Malaysia.

<sup>3</sup> College of Oil and Gas Engineering, Basrah University for Oil and Gas, 61004 Basrah, Iraq.

Email: azlinawati@ump.edu.my

**Abstract.** This contribution presents the characterization of poly(acrylamide-*co*-acrylic acid)-grafted-poly(styrene-*co*-methyl methacrylate) [poly(AAm-*co*-AAc)-*g*-poly(St-*co*-MMA)] The chemical structure of poly(AAm-*co*-AAc)-*g*-poly(St-*co*-MMA) microgels was proposed. The effect of MBA contents on the degree of cross-linking (%), water absorbency (EWC, %), glass transition temperature,  $T_g$  and thermal degradation were studied. The degree of cross-linking (%) and EWC, % increased at 1.5 to 1.675 wt.% of MBA might be due to mono cross-links of MBA. The fluctuation of  $T_g$  and melting temperature ( $T_m$ ) from 1.85 to 2.2 wt.% of MBA might be due to di, poly and cyclic cross-links of MBA. Decomposition of poly(AAm-*co*-AAc)-*g*-poly(St-*co*-MMA) was slightly affected by increasing in MBA contents from 1.5 to 2.2 wt.%.  $T_g$  of poly(AAm-*co*-AAc)-*g*-poly(St-*co*-MMA) was decreased at 1.5 to 1.675 wt.% of MBA due to increase in ordered structure and crystallinity content, which led to an increase in  $T_m$ .

**Keywords.** Microgels; Cross-linking; Emulsion; Core-shell; Network

## 1. Introduction

Microgels have become a very attractive research area combining at the same time fundamental and applied topics of great interest. Interest in microgels comes from their unique blend of properties with consistent multi useful aspects of conventional macrogels and colloidal dispersion [1]. Because of the versatility of these materials, there has been a growing interest in a development of more advanced architecture, hence are multifunctional. The advanced architecture is core-shell morphology, which offers potential applications in many fields, including drug delivery, controlled release, and sensors [2]. The microgels systems might combine the characteristics and properties of both shell and core. Furthermore, the surface properties of the hydrogels shell are translated to the core, imparting new functionality to the microgels [3].

Consequently, a fundamental understanding of the mechanism leading to the formation of the polymeric chains is very important to develop product design and manufacture. Cross-linker is



multifunctional monomer normally used in free-radical polymerization to construct network structure [4]. The concentration of cross-linker is mainly depending on polymerization technique with lower cross-linker content need to be used in emulsion polymerization than in bulk and solution polymerization. Furthermore, the semi-batch process used a lower concentration of cross-linkers than a batch process. In emulsion polymerization, cross-linker is used to control the particle morphologies and enhancement the product mechanical properties [5]. At present, the network structure within these microspheres is not well understood, and a precise control of the cross-linked network structure seems to be a formidable task except controlling the overall cross-linking density by changing the amount of cross-linking agent [6]. Thus, it is important to measure the optimum amount of cross-linker used and study the structure-properties relationship.

Degradation can affect the deterioration in polymer properties where it can be caused by heat, stress, and radiation due to a breakdown of its chemical structure [7]. The thermal gravimetric analysis is a simple and accurate method to determine polymers thermal stability. Knowledge of degradation and mode of decomposition under the influence of heat is highly recommendable in the processing and fabrication procedures. The threshold decomposition temperature indicates the highest fabrication temperature. Cross-linked networks have better thermal properties than corresponding homopolymers. This is usually, attributed to the networking of the phases [8].

Previously, the research of synthesis, characterization and morphology study of poly(AAm-co-AAc)-g-poly(St-co-MMA) “raspberry”- shape like structure microgels have been carried out. The evidence of the “raspberry”- shape like structure core microgels via electron microscopy have been shown [9]. In the present work, the effect of the cross-linker amount on cross-linked network structure, water absorbency and thermal properties of poly(AAm-co-AAc)-g-poly(St-co-MMA) microgels were investigated.

## 2. Materials and Methods

### 2.1. Materials

Acrylamide (AAm, 99%), methyl methacrylate (MMA, 99%), acrylic acid (AAc, 99%) and styrene (St, 99%) were used as monomers. *N,N'*-methylenebisacrylamide (MBA, 99%) was used as cross-linker. sodium dodecyl sulfate, (SDS, 99%), sorbitan monooleate (span 80) and octylphenol ethylene oxide, (Triton X-100) were used as surfactants. Potassium persulphate, (KPS, 99%) was used as the initiator. All of the materials were purchased from MERCK, Germany and used as received.

### 2.2. Microgels preparation

Poly(AAm-co-AAc)-g-poly(St-co-MMA) microgels were prepared via pre-emulsified semi-batch emulsion polymerization as reported in previous work [9].

### 2.3. Characterization

#### 2.3.1. Degree of cross-linking (%)

The degree of cross-linking (%) during the polymerization was carried out using an extraction method based on the polymer mass that remained after extraction with dimethylformamide (DMF). A pre-determined weight of dried microgel samples ( $0.3 \pm 0.05$  g) were immersed in DMF for a period of 15 hours at room temperature. The samples were filtered and dried in an oven at 80°C until a constant weight was obtained to ensure that all of the solvents was vaporized. The degree of cross-linking of the microgels films based on the total emulsion solids was calculated using Equation 3.1:

$$\text{Degree of cross-linking (\%)} = (W_1 / W_0) \times 100 \quad (3.1)$$

Where,  $W_1$  and  $W_0$  are the weight of dry microgels film after and before extraction, respectively [10].

### 2.3.2. Water Absorbency

The dried sample ( $0.3 \pm 0.05$  g) was immersed in 200 ml of distilled water at room temperature for a period of 24 hours. The equilibrium water content (EWC) was calculated using equation 3.2 [11]:

$$\text{EWC (\%)} = [(w_s - w_d) / w_s] \times 100 \quad (3.2)$$

Where  $w_s$ , is the weight of the swollen sample and  $w_d$  is the weight of the dry sample after swelling. All of the experiments were carried out five times repeatedly and the average values were reported.

### 2.3.3. Differential Scanning Calorimeter (DSC)

DSC was used to determine glass transition temperature,  $T_g$  of the microgels. DSC assessments were carried out according to ASTM D 3418 using Perkin Elmer DSC 7 (USA), at a heating rate of  $10^\circ\text{C}/\text{min}$  in the range of 30 to  $500^\circ\text{C}$ . Dried microgels film with the weight of 7-10 mg was placed in a sealed aluminum pan, and an empty aluminum pan was used as a reference.

### 2.3.4. Thermogravimetric Analysis (TGA)

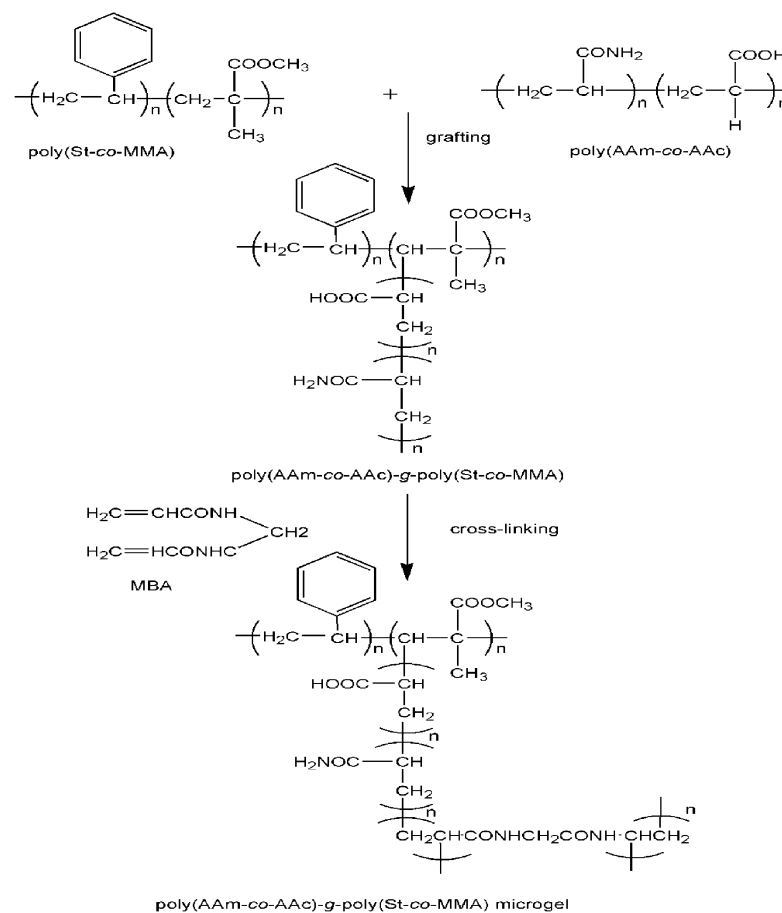
TGA was used to determine the thermal degradation of the microgels film. TGA assessments were carried out according to ASTM E 1131 using Perkin Elmer TGA 7 (USA). The dried microgels film was scanned from  $30$ - $950^\circ\text{C}$ , at a heating rate of  $10^\circ\text{C}/\text{min}$ . Each film was placed in an open platinum pan where nitrogen was used together as the purge gas at a flow rate of  $20$  mL/min. Onset temperature of a 10% and 75% weight loss deviation from the baseline of the thermogravimetric (TG) curve were used as an indicator for resulted products thermal stability.

## 3. Results and discussion

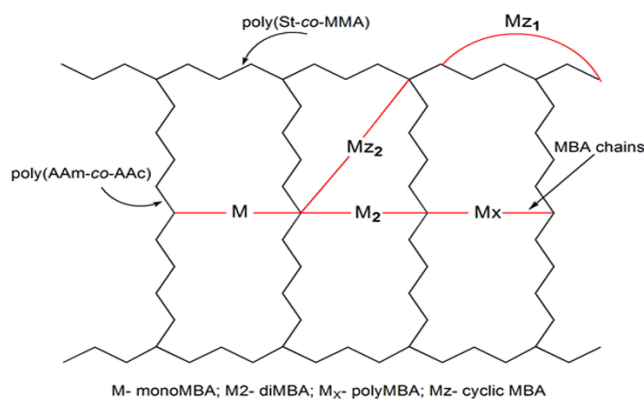
### 3.1. Proposed route

Figure 1 shows the proposed route to the formation of cross-linked network structure of poly (AAm-co-AAc)-g-poly (St-co-MMA) microgels based on mono cross-links of MBA. The polyfunctionality of MBA cross-linker which has four reactive sites that can be linked both sides to the poly(AAm-co-AAc)-g-poly(St-co-MMA) to form three dimensional (3D) network [12]. During emulsion polymerization persulfate radicals anion were formed and react with monomers dissolved in the aqueous phase to produce charged oligomers [13]. The polymerization was proceed in micelles and poly (AAm-co-AAc) and poly (St-co-MMA) were formed. Poly (AAm-co-AAc) is hydrophilic and poly (St-co-MMA) is hydrophobic. The difference in hydrophilicity between poly (AAm-co-AAc) and poly (St-co-MMA) led to form poly (AAm-co-AAc) seeds at an early stage of polymerization. After that, poly (AAm-co-AAc) particles were grafted with poly (St-co-MMA) core, adhere, and then coagulate to form the shell. The original seeds of poly (AAm-co-AAc) deformed from its original shape of a sphere into an outer shell then uniformly cross-linked with MBA. Thus, at a certain weight ratio of poly (AAm-co-AAc)-g-poly (St-co-MMA), microdomains have grown in size and joined together to form a “raspberry”-shape like structure core. Finally, these microdomains coalesce together to complete the shell formation of the “raspberry” particles [9].

Cross-linker acting as a bridge between the polymer chains by forming an equivalent bond from its reactive sites. Mono, di, poly, and cyclic cross-links might be formed inside the network structures of poly (AAm-co-AAc)-g-poly (St-co-MMA) microgels as illustrated in figure 2 Mono, di and poly cross-links occur between two different chains (intermolecular cross-linking). Furthermore, cyclizations occur in the single chain (intramolecular cross-linking). Primary cyclization ( $Mz_1$ ), occurring between the same growing primary chains, creating loops or cycles. Secondary cyclization ( $Mz_2$ ) occurring between the same macromolecule but belonging to a different primary chain [5].



**Figure 1.** The route to the formation of cross-linked network structure of poly (AAm-co-AAc)-g-poly (St-co-MMA) microgels.



**Figure 2.** Cross-linked network structure formed by mono, di, poly and cyclic MBA cross-links.

### 3.2. Degree of cross-linking (%) and Water Absorbency

Figure 3 shows the degree of cross-linking and EWC, % as a function of MBA amount for every batch of poly(AAm-co-AAc)-g-poly(St-co-MMA) microgels. It is clear that the cross-linking degree shared the same trend with EWC, %. Maximum EWC, 72.6 % was obtained at 1.675 wt.% of MBA, and it is decreased to 63.9 % at 1.85 wt.% of MBA. Decreasing in EWC, % at 1.85 wt.% of MBA might be as a result of the formation of di and poly cross-links, network space gets diminished and less water can

trap inside the microgels [14]. Moreover, further increases of MBA amount at 2.025 wt.% led to increasing EWC to 69 % due to the enhancement of the 3D network form which increase the amount of trapped water. However, further increases of MBA amount at 2.2 wt.%, produced tighter polymer network with decreasing the pores size and preventing the water to diffuse into the network structure and thus reduces the EWC, %. The water absorbency of the microgels film is the evidence that the hydrogels properties of poly(AAm-co-AAc) shell were translated to the poly(St-co-MMA) hydrophobic core.

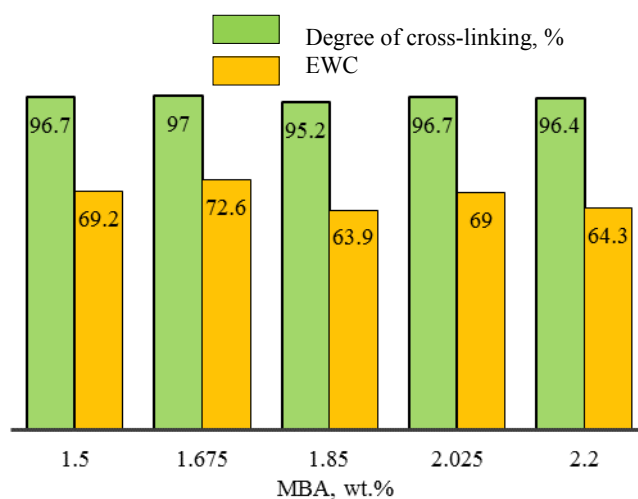


**Figure 3.** Cross-linking degree (%) and equilibrium water content (EWC, %) of poly(AAm-co-AAc)-g-poly(St-co-MMA) as a function of MBA contents.

### 3.3. Differential Scanning Calorimeter (DSC) Analysis

Figure 4 shows DSC curves of poly(AAm-co-AAc)-g-poly(St-co-MMA). Two distinct glass transitions temperature,  $T_g$  peaks were observed, and that the curve returns essentially to baseline values in between the two peaks is the evidence that the two polymers are highly phase separated copolymers, this result are similar to work reported by Stubbs [15]. The first transition representing the core of the microgels, poly(St-co-MMA) and the second ( $T_{g2}$ ) transition for the poly(AAm-co-AAc) shell. The results show that the of  $T_g$  of poly(AAm-AAc) (161°C) is higher than poly(St-co-MMA) (103°C). The value of both  $T_g$  is higher than theoretical  $T_g$  due to the cross-links structure of the microgels particles. It is well known that introducing cross-linkages into a polymer raises the glass temperature [16]. In addition, there is a decrease in the specific volume, since introducing cross-linkages involves the exchange of Van der Waals' bonds for shorter, more compact primary bonds. Thus, the process of cross-linking should affect the segmental mobility and the related properties in a manner similar to the effect of an increase in the molecular weight of the primary chains [17]. Furthermore, high  $T_g$  of poly(St-co-MMA) might be due to the thermal properties of poly(AAm-co-AAc) hydrogels shell were translated to the core. For each polymer phase, the change in the heat capacity across the  $T_g$  is representative of the amount of that phase [18]. The third transition shows the melting points ( $T_m$ ) of the film sample. The results in Table 1 indicated that  $T_{g1}$  and  $T_{g2}$  decreased and  $T_m$  increased with the increase in MBA amount from 1.5 wt.% to 1.675 wt.%. This might be due to a homogenous network of pores formed by mono cross-links led to enhance the ordered structure and crystallinity content consequently increases the  $T_m$  from 390 to 430°C. However, further increases of MBA amount from 1.85 to 2.2 wt.%, which results in fluctuation of  $T_g$  and  $T_m$  due to inefficient cross-linking which affected the 3D network. Furthermore, the formation of di, poly, and cyclic cross-links caused to produce heterogeneous network of pores which affected the thermal properties.

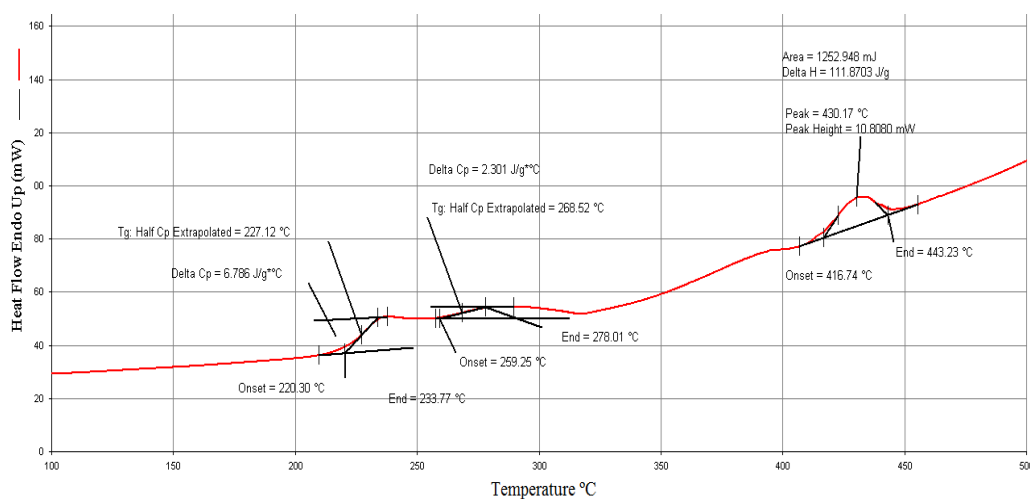


**Figure 4.** DSC trace for poly(AAm-co-AAc) hydrogels shell and poly(St-co-MMA) hydrophobic core.

**Table 1.** Glass transition temperatures,  $T_g$  and crystalline melting points,  $T_m$  of microgels with varying amount of MBA cross-linker.

MBA (pphm)	Exothermic		
	$T_{g1}$ (°C)	$T_{g2}$ (°C)	$T_m$ (°C)
1.500	235	270	390
1.675	227	269	430
1.850	238	266	430
2.025	228	297	385
2.200	226	292	431

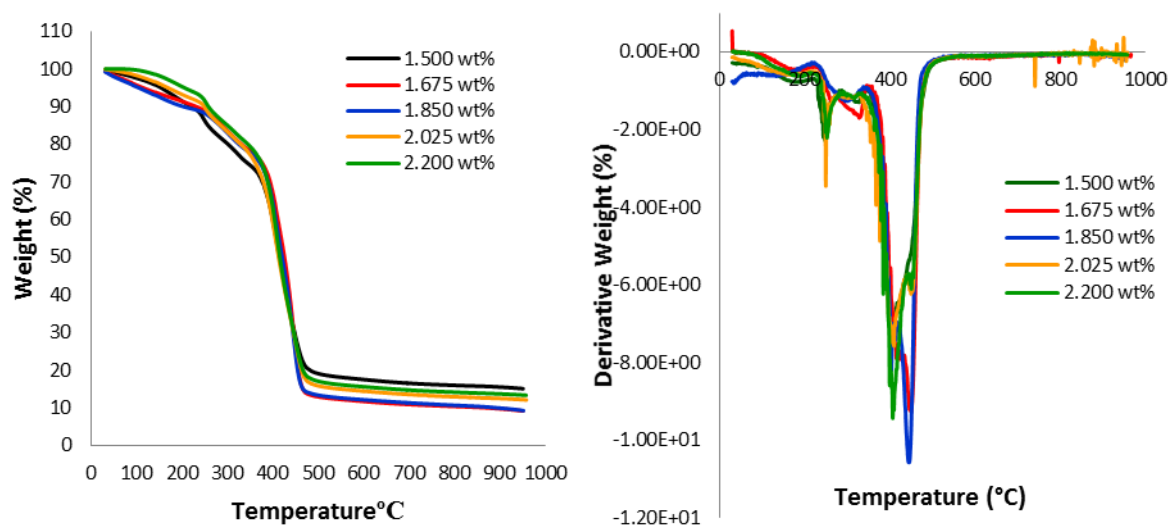
### 3.4. Thermal Gravimetric Analysis (TGA)

TGA data of poly(AAm-co-AAc)-g-poly(St-co-MMA) microgels with varying amount of MBA cross-linker are shown in Table 2. The data showed 10% ( $T_d$ ), 75% ( $T_{75\%}$ ) and the maximum ( $T_{max}$ ) weight loss temperature and their char residue at 600 °C. Generally, the results indicated high temperatures of  $T_{10\%}$  for all samples. Increasing in  $T_{10\%}$  weight loss is an indication of enhancement in thermal stability [19]. Increasing in  $T_{10\%}$  from 219 °C to 288 °C is due to the increase in MBA amount. When MBA amount was increased, more cross-linking points were generated to bond with polymer molecules. Furthermore, the intramolecular hydrogen bond within MBA units also increased consequently more heat was needed to break the structures.

In all cases, poly(AAm-co-AAc)-g-poly(St-co-MMA) microgels showed four steps of decomposition as shown in derivative thermal gravimetric (DTG) curves in figure 5 The first step below 100 °C is due to the removal of adsorbed water molecules [20]. The second step is about 249 to 260 °C might be due to the destruction of carbonyl groups (e.g., amide, carboxyl) [20, 21]. The third step is attributed to the main chain pyrolysis beginning at about 290 to 330 °C with the evolutions of aromatics from the degradation of styrene. Polystyrene degrades into a mixture of styrene (40%), toluene (2.4%), methyl styrene, etc. above 300°C [8, 20]. The last step weight loss was corresponding to degradation of the polymer backbones at about 404 to 445 °C [21]. At 600 °C, residue of poly(AAm-co-AAc)-g-poly(St-co-MMA) with varying contents of MBA cross-linker is about 10.12 to 17.55%. Depending on the mentioned results can be concluded that increasing in MBA amount slightly affected the decomposition of poly(AAm-co-AAc)-g-poly(St-co-MMA) microgels.

**Table 2.** TGA data of the poly(AAm-co-AAc)-g-poly(St-co-MMA) with varying amount of MBA.

MBA (pphm)	Temperature (°C)		Max wt. loss (%)	$T_{max}$ (°C)	Residue at 600 °C (%)
	$T_{10\%}$	$T_{75\%}$			
1.500	219	458	71.06	385.16	17.55
1.675	248	454	74.65	377.43	14.47
1.850	255	449	76.14	410.82	10.12
2.025	258	455	75.15	387.40	15.64
2.200	288	458	77.53	399.16	16.91

**Figure 5.** (A) TG Curves, and (B) DTG curves of poly(AAm-co-AAc)-g-poly(St-co-MMA) microgels showed four steps of decomposition.

#### 4. Conclusions

Poly(AAm-co-AAc)-g-poly(St-co-MMA) “raspberry”- shape like structure microgels with varying contents of MBA cross-linker were synthesized via pre-emulsified semi-batch emulsion polymerization. Variation of the cross-linker concentration provides good understanding relationships between the cross-linked structure and properties. The formation of cross-linked network structure of poly(AAm-co-AAc)-g-poly(St-co-MMA) microgels was proposed based on mono cross-links of MBA. 1.675 wt.% of MBA was suggested as the optimum amount of the cross-linker used. The maximum degree of cross-linking, % and EWC, % was achieved at 97 and 72.6% respectively. The water absorbency of the microgels film and high  $T_g$  of poly(St-co-MMA) core is the evidence that the properties of the hydrogels shell were translated to the hydrophobic core. Such structure-properties relationships are important for the design of future systems to use in potential applications such as medical devices coating.

#### Acknowledgment

The authors would like to thank to Universiti Malaysia Pahang and Universiti Teknologi Malaysia for the financial support under University Grant (No. RDU1703286).

**References.**

- [1] Ramli, R.A., W.A. Laftah, and S. Hashim, Core-shell polymers: a review. *Rsc Advances*, 2013. 3(36): p. 15543-15565.
- [2] Ramli, R.A., Hollow polymer particles: a review. *RSC Advances*, 2017. 7(83): p. 52632-52650.
- [3] Hendrickson, G.R., et al., Design of Multiresponsive Hydrogel Particles and Assemblies. *Advanced Functional Materials*, 2010. 20(11): p. 1697-1712.
- [4] Laftah, W.A., S. Hashim, and A.N. Ibrahim, Polymer Hydrogels: A Review. *Polymer-Plastics Technology and Engineering*, 2011. 50(14): p. 1475-1486.
- [5] Bouvier-Fontes, L., et al., Seeded Semicontinuous Emulsion Copolymerization of Butyl Acrylate with Cross-Linkers†. *Macromolecules*, 2005. 38(4): p. 1164-1171.
- [6] Tobita, H., Crosslinking kinetics in emulsion copolymerization. *Macromolecules*, 1992. 25(10): p. 2671-2678.
- [7] Shah, A.A., et al., Biological degradation of plastics: A comprehensive review. *Biotechnology Advances*, 2008. 26(3): p. 246-265.
- [8] Mathew, A.P., S. Packirisamy, and S. Thomas, Studies on the thermal stability of natural rubber/polystyrene interpenetrating polymer networks: thermogravimetric analysis. *Polymer Degradation and Stability*, 2001. 72(3): p. 423-439.
- [9] Ramli, R.A., S. Hashim, and W.A. Laftah, Synthesis, characterization, and morphology study of poly(acrylamide-co-acrylic acid)-grafted-poly(styrene-co-methyl methacrylate) “raspberry”-shape like structure microgels by pre-emulsified semi-batch emulsion polymerization. *Journal of Colloid and Interface Science*, 2013. 391(0): p. 86-94.
- [10] Xie, F., Z.-H. Liu, and D.-Q. Wei, Curing Kinetic and Properties of Acrylic Resin Cured with Aziridine Crosslinker. *Chinese Journal of Polymer Science*, 2002. 20(1): p. 65-70.
- [11] Rodkate, N. and M. Rutnakornpituk, Multi-responsive magnetic microsphere of poly (N-isopropylacrylamide)/carboxymethylchitosan hydrogel for drug controlled release. *Carbohydrate Polymers*, 2016.
- [12] Singh, B. and N. Chauhan, Modification of psyllium polysaccharides for use in oral insulin delivery. *Food Hydrocolloids*, 2009. 23(3): p. 928-935.
- [13] Young, R.J., and Lovell, P. A. , Introduction to Polymers. 1991: Chapman and Hall: Kluwer Academic Publisher.
- [14] Wu, J., et al., Study on starch-graft-acrylamide/mineral powder superabsorbent composite. *Polymer*, 2003. 44(21): p. 6513-6520.
- [15] Stubbs, J.M. and D.C. Sundberg, A round robin study for the characterization of latex particle morphology—multiple analytical techniques to probe specific structural features. *Polymer*, 2005. 46(4): p. 1125-1138.
- [16] Loshaek, S., Crosslinked polymers. II. Glass temperatures of copolymers of methyl methacrylate and glycol dimethacrylates. *Journal of Polymer Science*, 1955. 15(80): p. 391
- [17] Fox, T.G. and S. Loshaek, Influence of molecular weight and degree of crosslinking on the specific volume and glass temperature of polymers. *Journal of Polymer Science*, 1955. 15(80): p. 371-390.
- [18] Sundberg, D.C. and Y.G. Durant, Latex Particle Morphology, Fundamental Aspects: A Review. *Polymer Reaction Engineering*, 2003. 11(3): p. 379-432.
- [19] Yu, Y.-Y. and W.-C. Chen, Transparent organic-inorganic hybrid thin films prepared from acrylic polymer and aqueous monodispersed colloidal silica. *Materials Chemistry and Physics*, 2003. 82(2): p. 388-395.
- [20] Ding, R., et al., Preparation and characterization of polystyrene/graphite oxide nanocomposite by emulsion polymerization. *Polymer Degradation and Stability*, 2003. 81(3): p. 473-476.
- [21] Liu, Y.-L., C.-Y. Hsu, and K.-Y. Hsu, Poly(methylmethacrylate)-silica nanocomposites films from surface-functionalized silica nanoparticles. *Polymer*, 2005. 46(6): p. 1851-1856.